Available online at www.sciencedirect.com
SCIENCE DIRECT
Journal of Catalysis 230 (2005) 75–85
JOURNAL OF CATALYSIS
www.elsevier.com/locate/jcat

Influence of reduction temperature on the catalytic behavior of Co/TiO_2 catalysts for CH_4/CO_2 reforming and its relation with titania bulk crystal structure

Kazuhiro Takanabe [a], Katsutoshi Nagaoka [b,1], Kentaro Nariai [a], Ken-ichi Aika [a,b,*]

[a] *Department of Environmental Chemistry and Engineering, Interdisciplinary Graduate School of Science and Engineering, Tokyo Institute of Technology, 4259 Nagatsuta, Midori-ku, Yokohama 226-8502, Japan*
[b] *CREST, JST (Japan Science and Technology Corporation), Japan*

Received 17 July 2004; revised 10 October 2004; accepted 2 November 2004

Available online 28 December 2004

Abstract

The influence of reduction temperature on the catalytic behavior of 10 wt% Co/TiO_2 catalysts, for CO_2 reforming of methane to synthesis gas under atmospheric pressure, was investigated. Co/TiO_2-anatase catalysts reduced at lower temperatures ($\leqslant$ 1073 K) showed stable activities. On the other hand, the catalyst reduced at higher temperatures ($\geqslant$ 1123 K), where the crystal phase of TiO_2 is transformed from anatase to rutile during the reduction, provided almost no activity. In addition, Co/TiO_2-rutile also showed very low activity, regardless of the reduction temperature. No carbon deposition ($<$ 0.01 wt%) was observed for any of the Co/TiO_2 catalysts. XPS and XRD analysis revealed that the main cause of low activity and deactivation of the catalyst was the oxidation of metallic cobalt. Experimental observations suggest that the large difference in initial activity corresponds to the different crystal structure of TiO_2 after reduction.

Keywords: Co/TiO_2; Methane dry reforming; Influence of reduction temperature; Strong resistance to coking; Strong metal support interaction; Crystal structure of TiO_2; Anatase; Rutile

1. Introduction

CO_2 reforming of methane to synthesis gas ($CH_4 + CO_2 \rightleftarrows 2CO + 2H_2$) has been a topic of considerable interest for natural gas conversion. It is well known that deposition of carbonaceous species on catalysts is a serious issue for the reaction, causing catalyst deactivation and pressure drop due to plugging of the reactor [1]. Carbon originates mainly from two reactions: CH_4 decomposition ($CH_4 \rightarrow C + 2H_2$) and CO disproportionation ($2CO \rightarrow C + CO_2$) [2]. One of the mechanisms proposed for the reforming of hydrocarbons suggests that the hydrocarbon is dissociatively adsorbed on metallic sites, whereas CO_2 is adsorbed on the support and the adsorbed oxygen species derived from CO_2 on the support reacts with the adsorbed carbon species derived from hydrocarbon on the metal [3,4]. To minimize the deposition of carbon on the catalyst, it has been suggested that the catalyst should be designed to avoid large ensembles of the metal species that facilitates carbon formation [2] and to enhance sorption of oxidants (i.e., CO_2 and H_2O) on the support that can remove the deposited carbon formed on the metal [5,6].

In general, supported noble metals, such as Rh, Ru, Pd, Pt, and Ir, can lead to lower carbon deposition in the CH_4/CO_2 reaction [2]. However, from a practical point of view, noble metals are unsuitable for industrial use, considering their high cost and restricted availability. Supported Ni catalysts are commonly studied because of their low cost; however, nickel can easily induce carbon deposition. Although cobalt catalysts have not been a focus of attention

* Corresponding author. Fax: +81 45 924 5441.
E-mail addresses: takanabe@chemenv.titech.ac.jp (K. Takanabe), nagaoka@cc.oita-u.ac.jp (K. Nagaoka), nariai@chemenv.titech.ac.jp (K. Nariai), kenaika@chemenv.titech.ac.jp (K. Aika).
[1] Present address: Department of Applied Chemistry, Faculty of Engineering, Oita University, Dannoharu 700, Oita 870-1192, Japan.

0021-9517/$ – see front matter
doi:10.1016/j.jcat.2004.11.005

until recently, it has been revealed that Co/MgO [7] and Co/Al_2O_3 [8] showed considerable activity for the CH_4/CO_2 reaction, which suggests that cobalt could be a suitable metal.

In agreement with the mechanism mentioned above, a number of contributors have suggested that the nature of the support strongly affects the catalytic behavior and carbon deposition in the CH_4/CO_2 reaction [2]. Among oxide supports, TiO_2 [3,9–17] and ZrO_2 [4,18–22], which are known to show strong interaction with the catalytic metal [23–25], effectively suppress carbon deposition. The proposed mechanism [3,4,21] suggests that, by H_2 reduction, partially reduced oxide species, such as TiO_x and ZrO_x, migrate onto the metal particles to destroy large ensembles of the metal and enhance the extent of the active interfacial region between the metal and support. In this respect, pretreatment of TiO_2- or ZrO_2-supported catalysts with H_2 can directly change the nature of the support at the perimeter of the metal, which is assumed to be the active site for CH_4/CO_2 reforming.

It should also be mentioned that TiO_2 has two kinds of stable crystal structures, anatase and rutile. The anatase phase is irreversibly transformed to rutile at high temperature. Studies of adsorption and reaction of CO [26–28] and alcohol [29,30] on TiO_2 suggested that the different bulk crystal structures of TiO_2 influence the adsorption properties and catalytic activities for the reactions. However, little is known about the influence of the structural phase of TiO_2 in the CH_4/CO_2 reaction.

The authors have studied Co/TiO_2 catalysts for high-pressure CH_4/CO_2 reforming, where coke formation is highly favorable [15–17]. The catalytic behavior significantly depended on the H_2 reduction temperature, reaction pressure, and possibly the phase composition of TiO_2 (i.e., anatase and rutile) [15,16]. The optimized pretreatment provides the catalyst with a strong resistance to coke formation during the reaction, even at 2.0 MPa. However, because a low loading of Co is essential for stable operation at high pressure [15] and because of the practical difficulties of characterizing the catalysts in a high-pressure flow system, the nature of the Co/TiO_2 catalyst has not been well elucidated. In this contribution, the catalytic behavior and nature of Co/TiO_2 catalysts for CH_4/CO_2 reforming at atmospheric pressure will be discussed thoroughly. Prior to kinetic measurements, catalysts prepared with TiO_2, occurring only in the anatase or rutile phase, have been reduced in H_2 at different temperatures. To determine the parameters that influence catalytic behavior and deactivation, extensive characterization has been performed.

2. Methods

2.1. Catalyst preparation

Two types of TiO_2 were obtained by calcination of TiO_2 (Ishihara Sangyo, A-100) at 773 K (anatase phase, denoted TiO_2(a)) and at 1373 K (rutile phase, denoted TiO_2(r)). The phase compositions were confirmed by X-ray diffraction (XRD) analysis. The BET surface areas of TiO_2(a) and TiO_2(r) were 11 and 2 $m^2\,g^{-1}$, respectively.

Co/TiO_2(a) and Co/TiO_2(r) were prepared by incipient wetness impregnation with the use of either TiO_2(a) or TiO_2(r) and an aqueous solution of $Co(NO_3)_2 \cdot 6H_2O$. Cobalt loading was set to 10 wt%. The catalysts were dried at room temperature and then at 373 K overnight, followed by calcination at 673 K for 4 h to remove ligands from the cobalt precursor. The powder-form catalysts were pressed into pellets, crushed, and sieved to obtain grains with diameters between 600 and 900 μm.

2.2. CH_4/CO_2 reaction

All catalysts were tested at atmospheric pressure. Typically, 0.1–1.0 g of the catalyst was loaded into a fixed-bed tubular inconel reactor (ID 6 mm) that was passivated with alumina. The reactor was operated in an up-flow mode with the catalyst bed held between quartz wool plugs. Before the reaction, the catalysts were reduced in situ with a H_2 flow (25 ml min^{-1}) at various temperatures in the range of 973–1223 K. The required temperature was reached at a rate of 10 K min^{-1} and maintained for 1 h. After reduction, H_2 was purged with a flow of He gas, and the reactor was then set to a reaction temperature of 1023 K. CH_4/CO_2 gases were passed through a bypass of the reactor to measure the exact feed composition and subsequently introduced into the catalyst bed at a total flow rate of 20–100 ml min^{-1} (space velocity (SV) = 1200–60,000 ml $g_{cat}^{-1}\,h^{-1}$). An ice-cold trap was set between the reactor exit and a gas chromatograph (GC), to remove water formed during the reaction. The reactants and products were analyzed with an on-line GC (Aera, M-200) equipped with a Porapak Q column, Molecular Sieve 5A column, and two thermal conductivity detectors (TCDs). After the reaction, the reactant gas was replaced with He at the reaction temperature, and subsequently the catalysts were cooled to room temperature for characterization. A blank test in the absence of the catalyst revealed no yield of CO or H_2.

The exit composition of the gases, at the initial stage of the reaction, was continuously monitored by a quadrupole mass spectrometer (Q-MS), M-QA200TS from ANELVA. The m/e values of 2 (H_2), 16 (CH_4), 28 (CO), and 44 (CO_2) were used. The intensities for all gases were calibrated with the GC after stable catalytic activities were obtained. The contribution of CO_2 fragmentation to CO ($m/e = 28$) was appropriately taken into account.

2.3. Catalyst characterization

X-ray photoelectron spectroscopy (XPS) was performed with an ULVAC-PHI Model 3057 ESCA system and monochromated Al-K_α (1486.7 eV, 200 W) under a pressure of

approximately 10^{-9} Torr. Samples were pressed into pellets and treated in the desired gas atmosphere and temperature. After each treatment, the pellets were purged in Ar and closed in glass capsules, then transferred into the spectrometer system without exposure to the ambient air. The measurements were carried out under approximately 1.0×10^{-6} Pa, with the C1s peak at 284.8 eV as a reference. To compensate for the loss of electrons during the measurements, a pass energy of 23.5 eV was used for all samples.

XRD analysis was performed with a Rigaku Multiflux X-ray diffractometer with monochromatized Cu-K_α. Metal crystallite sizes were calculated from line broadening with the Scherrer equation [31].

Quantification of deposited carbon was achieved by a temperature-programmed oxidation (TPO) method. After the reaction, the catalyst was heated to 1273 K, at a heating rate of 10 K min^{-1}, in an O_2/He mixture (5/95 vol/vol with a total flow of 50 ml min^{-1}). CO_x gases derived from deposited carbon were monitored with a methanator and a flame ionization detector (FID).

The specific surface area of the catalysts after H_2 reduction was determined by the BET method. The amounts of chemisorbed CO were determined by a pulse injection method. Typically, 0.1 g of catalyst was reduced in situ at the required temperatures for 1 h in a H_2 flow and flushed with He (> 99.999% purity) for 15 min at each temperature. Pulses of 1.08 ml containing 1% CO in He were injected over the catalysts at room temperature until no further adsorption of CO was detected with a TCD. Dispersion of the metal was calculated with the assumption of a 1:1 Co:CO stoichiometry.

Temperature-programmed reduction (TPR) measurements were carried out over 0.1 g of calcined catalyst from room temperature to 1223 K, at a rate of 10 K min^{-1} in flowing H_2/Ar gas mixture (5/95 vol/vol with a total flow of 30 ml min^{-1}). The hydrogen consumption was monitored with a TCD. A water-trap column was placed after the reactor to remove the water formed during the TPR.

TPO of the reduced catalyst was carried out with the use of CO_2 to investigate oxidation behavior. The temperature was increased from room temperature to 1223 K at a rate of 10 K min^{-1}. The increase in the catalyst weight during oxidation of the reduced catalyst in flowing CO_2 was monitored by differential thermogravimetry (SSC/5200, SII).

3. Results

3.1. Catalytic behavior of the Co/TiO$_2$ catalysts

Fig. 1 shows CH_4 conversions versus time on stream over the Co/TiO$_2$(a) catalysts reduced at different temperatures at SV of 6000 ml g$_{cat}^{-1}$ h^{-1}. Conversions of CH_4 and CO_2 for the Co/TiO$_2$(a) and Co/TiO$_2$(r) are listed in Table 1. From Fig. 1, it is obvious that the activities of Co/TiO$_2$(a) decreased with increasing reduction temperature. The catalysts

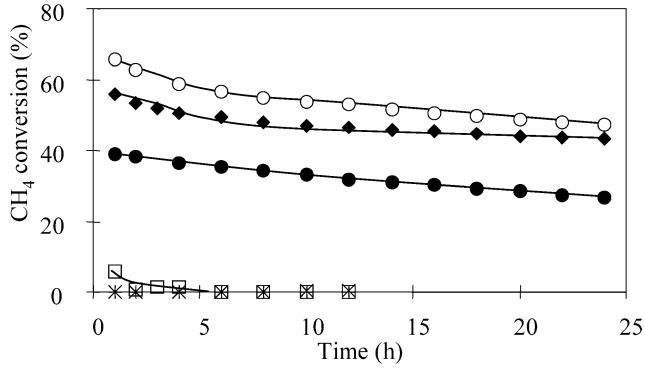

Fig. 1. CH_4 conversion vs. time on stream for Co/TiO$_2$(a) reduced at various temperatures. Reduction temperature: (○) 973 K; (◆) 1023 K; (●) 1073 K; (□) 1123 K; (×) 1173 K; (+) 1223 K. (Reaction conditions: $CH_4/CO_2 = 1$; 1023 K; 0.1 MPa; SV = 6000 ml g$_{cat}^{-1}$ h^{-1}.)

reduced at 973–1073 K showed relatively high CH_4 conversions and became only slightly deactivated with prolonged usage. On the other hand, the catalysts reduced at 1123–1223 K showed fairly low activity from the beginning of the reaction. The activities for the Co/TiO$_2$(r) catalysts reduced within the temperature range of 973–1123 K were all very low from the initial stage of the reaction (Table 1).

Fig. 2 shows the relative gas compositions for exit gases monitored by Q-MS as a function of time, focusing on the initial time on stream (< 60 s). For the Co/TiO$_2$(a) catalyst reduced at 1023 K (I), after the reactant gases were introduced into the reactor, concentrations for all of the gas components including reforming products, CO and H_2, increased and remained stable during the measurements, indicating consistency with the reforming shown in Fig. 1. On the other hand, for the Co/TiO$_2$(a) catalyst reduced at 1173 K (II) and the Co/TiO$_2$(r) catalyst reduced at 1023 K (III), the concentrations of the reforming products, CO and H_2, increased only initially and decreased rapidly to a very low level (20–40 s in Fig. 2 (II) and (III)). The decreases in CO and H_2 occurred simultaneously with increases in CH_4 and CO_2. These phenomena indicate that reforming proceeded only slightly at the beginning of the reaction, and almost all catalytic activity was lost immediately. The concentration of CH_4 increased more rapidly than that of CO_2, indicating greater consumption of CO_2 than of CH_4. It should be noted that CO and H_2 were still produced after deactivation of the catalyst. This suggests that the reaction proceeds, however, only in small quantity.

The Co/TiO$_2$(a) catalysts reduced at 973–1073 K showed relatively stable activities (Fig. 1). Therefore, activity tests for the Co/TiO$_2$(a) catalyst reduced at 1023 K were performed over a wide range of SV (1200–60,000 ml g$_{cat}^{-1}$ h^{-1}). Fig. 3 shows CH_4 conversions versus time on stream at SV of 1200, 6000, and 60,000 ml g$_{cat}^{-1}$ h^{-1}. The conversion percentages are listed in Table 1. The CH_4 conversion increased with decreasing SV as expected. However, the equilibrium values for conversions (83.5% for CH_4) and yields were not obtained even at the lowest SV of 1200 ml g$_{cat}^{-1}$ h^{-1}. At this

Table 1
Conversions, yields and coke amounts for Co/TiO_2(a) and Co/TiO_2(r) reduced at various temperatures

Catalyst	Reduction temperature (K)	Space velocity (ml g_{cat}^{-1} h^{-1})	Time (h)	Conversion (%)		Coke amount (wt%)
				CH_4	CO_2	
Co/TiO_2(a)	973	6000	1	65.5	71.7	
			24	47.1	58.4	n.d.[a]
	1023	1200	1	80.2	81.9	
			50	59.8	66.6	n.d.[a]
		6000	1	55.7	64.3	
			24	43.4	54.7	n.d.[a]
		60,000	1	20.5	33.1	
			24	n.d.	n.d.	0.02
	1073	6000	1	39.0	51.2	
			24	26.5	38.9	n.d.[a]
	1123	6000	1	5.6	9.2	
			12	n.d.	n.d.	n.d.[a]
	1173	6000	1	0.1	2.0	
			12	n.d.	n.d.	n.d.[a]
	1223	6000	1	n.d.	0.2	
			12	n.d.	n.d.	n.d.[a]
Co/TiO_2(r)	973	6000	1	2.4	5.4	
			12	n.d.	n.d.	n.d.[a]
	1023	6000	1	0.8	2.0	
			12	n.d.	n.d.	n.d.[a]
	1123	6000	1	n.d.	n.d.	
			12	n.d.	n.d.	n.d.[a]

[a] n.d. (not detected) is below 0.01 wt%.

SV, deactivation was pronounced at the beginning of the reaction (within 6 h) but was suppressed with time. At a SV of 60,000 ml g_{cat}^{-1} h^{-1}, the catalyst initially showed reforming activity (CH_4 conversion: 20.5%). However, the catalyst gradually lost activity with time and completely within 20 h.

3.2. Characterization of the Co/TiO_2 catalysts

First, the TPO results revealed that no carbon was detected (< 0.01 wt%) for any of the Co/TiO_2 catalysts after the CH_4/CO_2 reaction (see Table 1).

The Co 2*p* XP spectra for the Co/TiO_2(a) catalysts reduced at 1023 and 1123 K, before and after reaction (1 h), are shown in Fig. 4. Peaks located at 777.4 and 777.5 eV, characteristic for metallic cobalt, appeared for the catalysts reduced at 1023 and 1123 K, respectively. For the catalyst reduced at 1023 K, smaller intensity peaks in the 779.5–781 eV region, attributed to an oxide phase of cobalt, were also observed. A peak at 777.2 eV, which can be assigned to metallic cobalt, remained after the reaction. However, a large shift of this peak to 780.1 eV was observed for the catalyst reduced at 1123 K. This indicates that metallic cobalt was oxidized during the CH_4/CO_2 reaction.

Fig. 5 shows the XRD patterns of the Co/TiO_2(a) catalysts (I) reduced at 1023–1173 K, before the CH_4/CO_2 reaction, and (II) after the CH_4/CO_2 reaction, respectively. Prior to the CH_4/CO_2 reaction (see Fig. 5 (I)), the metallic cobalt phase was observed for all of the catalysts (see the expanded scale on the right of Fig. 5). In addition, a slight phase transfer of TiO_2 from anatase to rutile was observed at 1073 K and predominantly so at 1123–1223 K. After the reaction (see Fig. 5 (II)), the metallic cobalt phase remained in the catalysts reduced at 973–1073 K, with higher intensities than those before the reaction. However, for the catalysts reduced at 1123–1223 K, the peak intensities for Co^0 decreased slightly during the reaction, and, instead, a $CoTiO_3$ phase was formed. Similarly, in the XRD pattern of the Co/TiO_2(a) catalyst after the reaction at a SV of 60,000 ml g_{cat}^{-1} h^{-1}, the $CoTiO_3$ phase was observed with small intensity, as shown in Fig. 5 (II) (A′). On the other hand, for the XRD pattern of the catalyst after reaction at a SV of 1200 ml g_{cat}^{-1} h^{-1} (not shown), the $CoTiO_3$ phase was not observed as it was for a SV of 6000 ml g_{cat}^{-1} h^{-1} (Fig. 5 (II)). The XRD patterns of the Co/TiO_2(a) catalysts reduced at 973 and 1223 K, before and after reaction, were similar to those of the catalysts reduced at 1023 K (A) and 1173 K (D), respectively (hence, these are excluded from the figures). With respect to Co/TiO_2(r), the XRD results displayed a tendency similar to that of the Co/TiO_2(a) catalyst reduced at 1173 K before and after the reaction (not shown).

Physicochemical properties of the catalysts are compiled in Table 2. For Co/TiO_2(a), the specific surface area decreased with increasing reduction temperature. The specific surface area decreased drastically with the reduction at 1123 K, which corresponds to the predominant phase transition of TiO_2 from anatase to rutile. For Co/TiO_2(r), the specific surface areas were the same for catalysts reduced at 973–1123 K, because of the strongly sintered structure of TiO_2(r) after calcination at 1373 K.

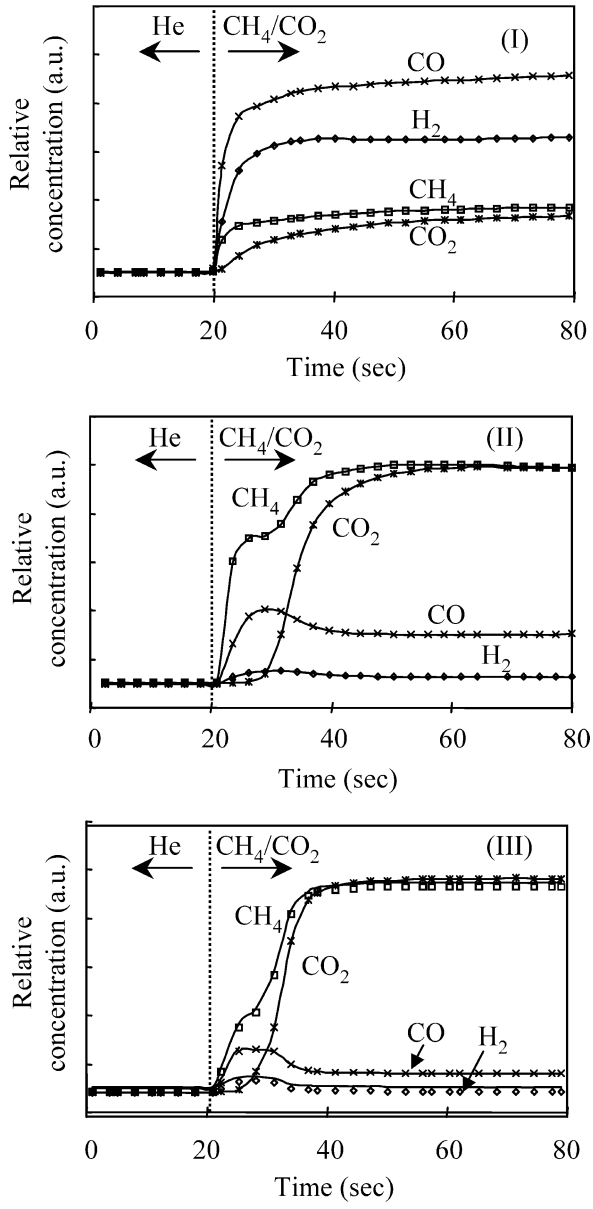

Fig. 2. Relative intensity of the exit gases at the initial stage of the reaction. (I) Co/TiO_2(a) reduced at 1023 K; (II) Co/TiO_2(a) reduced at 1173 K; (III) Co/TiO_2(r) reduced at 1023 K.

Dispersion of cobalt was evaluated by CO pulse chemisorption measurements. For Co/TiO_2(a), the dispersion of cobalt decreased with increasing reduction temperature up to 1073 K (0.36 to 0.11%) and then remained comparable above 1073 K (between 0.06 and 0.12%). For Co/TiO_2(r), dispersion of cobalt decreased gradually with increasing reduction temperature from 973 to 1123 K. It should be mentioned that the dispersions for Co/TiO_2(r) catalysts reduced at 973 (0.22%) and 1023 K (0.19%) were lower than those for the Co/TiO_2(a) catalysts reduced at 973 (0.36%) and 1023 K (0.30%), but higher than those for the Co/TiO_2(a) catalyst reduced at 1073–1223 K ($\leqslant 0.12\%$).

The cobalt metal crystallite sizes for the reduced catalysts were evaluated from XRD line broadening. Compara-

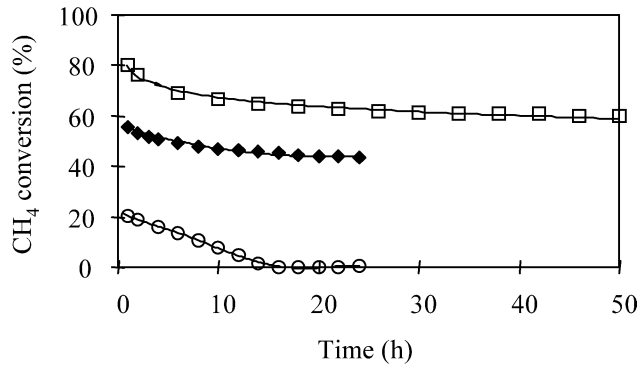

Fig. 3. CH_4 conversion vs. time on stream for Co/TiO_2(a) reduced at 1023 K with different SV: (□) 1200 ml g_{cat}^{-1} h^{-1}; (◆) 6000 ml g_{cat}^{-1} h^{-1}; (○) 60,000 ml g_{cat}^{-1} h^{-1}. (Reaction conditions: $CH_4/CO_2 = 1$; 1023 K; 0.1 MPa.)

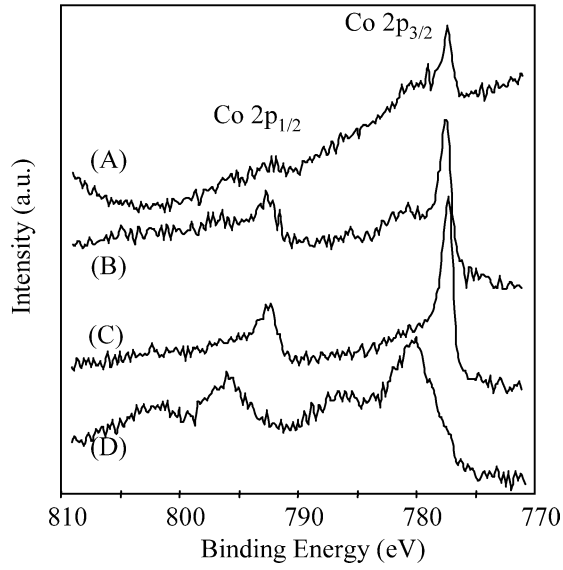

Fig. 4. XP spectra of (A) Co/TiO_2(a) reduced at 1023 K before reaction, (B) Co/TiO_2(a) reduced at 1023 K after reaction, (C) Co/TiO_2(a) reduced at 1123 K before reaction, and (D) Co/TiO_2(a) reduced at 1123 K after reaction. (Reaction conditions: $CH_4/CO_2 = 1$; 1023 K; 0.1 MPa, 1 h.)

ble values (26–35 nm) were obtained for all of the catalysts, regardless of the support phase composition. For all catalysts, the cobalt crystallite sizes increased slightly during the reaction at 6000 ml g_{cat}^{-1} h^{-1}, indicating that the cobalt particles experienced moderate sintering. It should be noted that the peak intensities for metallic cobalt, in Co/TiO_2(a) reduced at 1123–1223 K and Co/TiO_2(r), decreased after the reaction, and formation of $CoTiO_3$ was observed for these catalysts. For the Co/TiO_2(a) catalysts reduced at 1023 K, the crystallite size after the reaction (39 nm) at a SV of 1200 ml g_{cat}^{-1} h^{-1}, was distinguishably larger than before the reaction (26 nm), indicating that the catalyst had undergone sintering. For the catalyst after the reaction at a SV of 60,000 ml g_{cat}^{-1} h^{-1}, the formation of the $CoTiO_3$ phase was accompanied by a decrease in the intensity of the Co metallic phase.

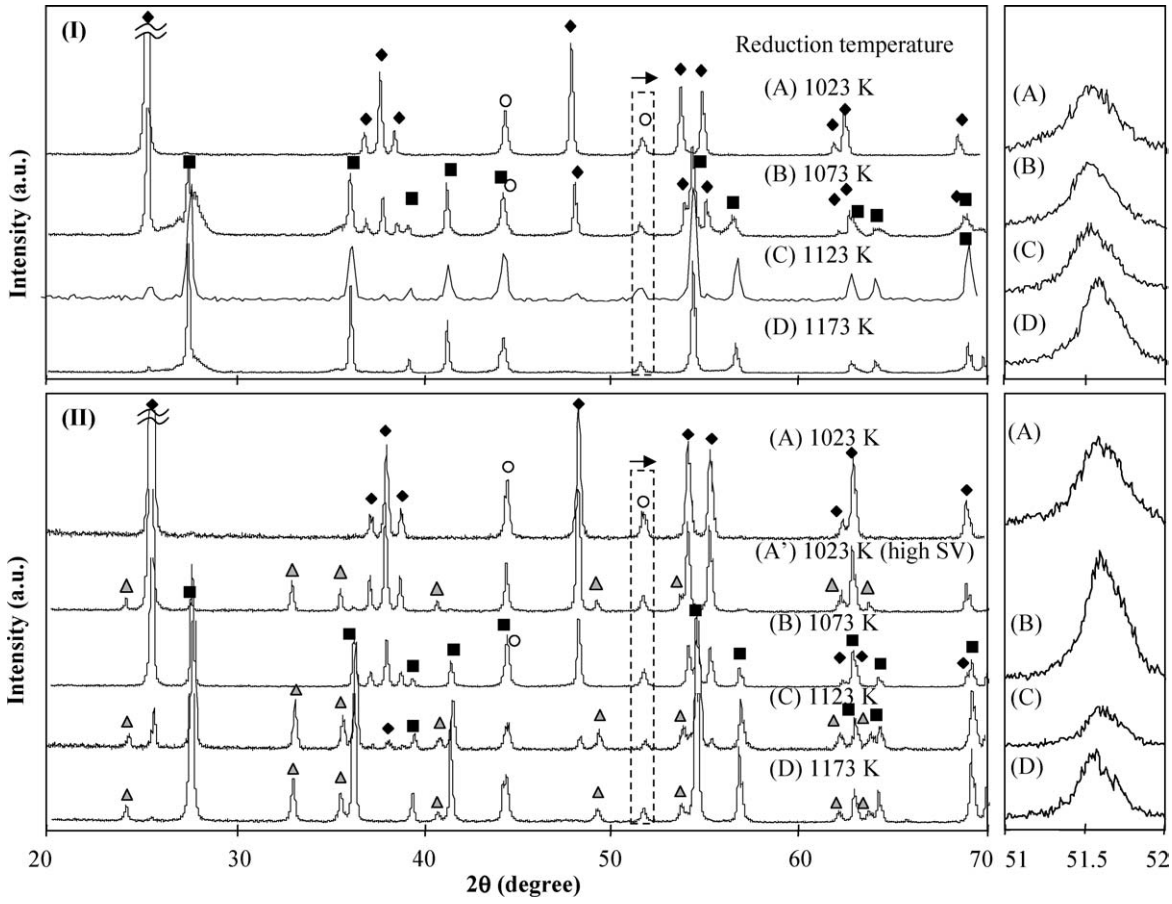

Fig. 5. XRD patterns for Co/TiO_2(a) reduced at different temperatures. (I) after the reduction, (II) after the reaction. Right box shows narrow scanning diffraction peaks for Co(200). Reduction temperature: (A), (A′) 1023 K; (B) 1073 K; (C) 1123 K; (D) 1173 K. (○) Co^0; (▲) $CoTiO_3$; (◆) TiO_2-anatase; (■) TiO_2-rutile. (Reaction conditions: $CH_4/CO_2 = 1$; 1023 K; 0.1 MPa. SV = 6000 ml g_{cat}^{-1} h^{-1}, except (A′) 60,000 ml g_{cat}^{-1} h^{-1}.)

Table 2
Specific surface area, metal surface area, and Co^0 crystallite size for Co/TiO_2(a) and Co/TiO_2(r) reduced at various temperatures

Reduction temperature (K)	Specific surface area[a] (m^2 g_{cat}^{-1})	CO adsorption[a] (μmol g_{cat}^{-1})	Cobalt dispersion (%)	Space velocity (ml g_{cat}^{-1} h^{-1})	Co crystallite size[b] (nm)	
					Before[a]	After[c]
			Co/TiO_2(a)			
973	11	6.07	0.36	6000	30	32
1023	10	5.07	0.30	1200	26	39
				6000	26	28
				60,000	26	38[d]
1073	9	1.80	0.11	6000	30	35
1123	5	1.08	0.06	6000	33	41[d]
1173	5	1.48	0.09	6000	34	37[d]
1223	3	2.00	0.12	6000	33	43[d]
			Co/TiO_2(r)			
973	2	3.70	0.22	6000	29	–[d]
1023	2	3.16	0.19	6000	29	–[d]
1123	2	1.44	0.08	6000	35	–[d]

[a] Before CH_4/CO_2 reaction (after reduction).
[b] Calculated from line broadening applying the Scherrer's equation [31].
[c] After CH_4/CO_2 reaction.
[d] $CoTiO_3$ phase was formed.

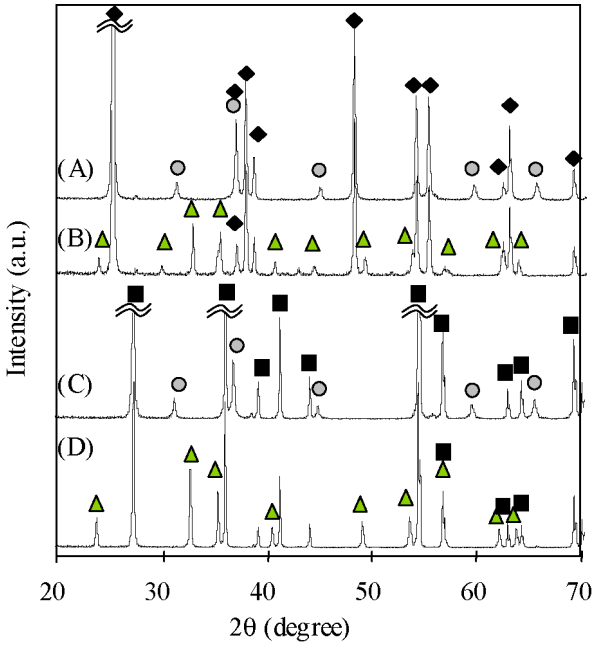

Fig. 6. XRD patterns for Co/TiO_2(a) and Co/TiO_2(r) after different treatments. (A) Co/TiO_2(a) after calcination at 673 K (before reduction); (B) Co/TiO_2(a) after CO_2/He treatment at 1023 K following the reduction at 1023 K; (C) Co/TiO_2(r) after calcination at 673 K (before reduction); (D) Co/TiO_2(r) after CO_2/He treatment at 1023 K following reduction at 1023 K. (●) Co_3O_4; (▲) $CoTiO_3$; (◆) TiO_2-anatase; (■) TiO_2-rutile.

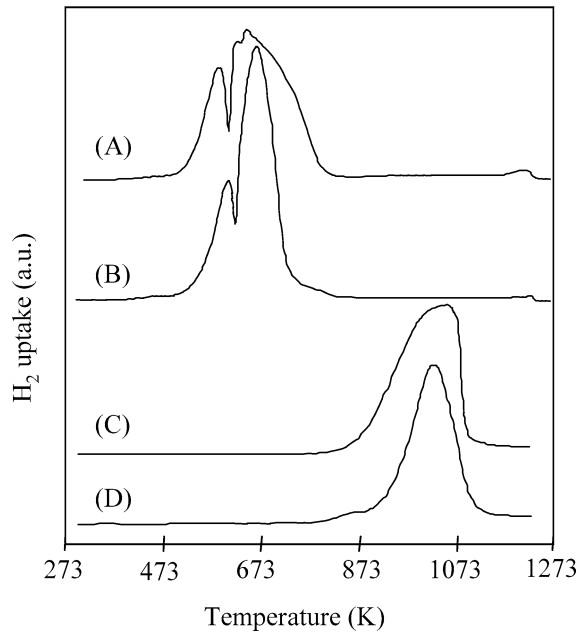

Fig. 7. TPR profiles for (A) Co/TiO_2(a) calcined at 673 K, (B) Co/TiO_2(r) calcined at 673 K, (C) Co/TiO_2(a) oxidized in CO_2/He at 1023 K, and (D) Co/TiO_2(r) oxidized in CO_2/He at 1023 K.

To follow the changes in the catalyst structure during the reduction, we carried out XRD analyses and TPR measurements. Figs. 6A and C show the XRD patterns of Co/TiO_2(a) and Co/TiO_2(r) calcined at 673 K (before reduction). These patterns indicate that cobalt was present as an oxide, Co_3O_4, after calcination at 673 K for both anatase and rutile phases. Figs. 7A and B show TPR profiles of the calcined Co/TiO_2(a) and Co/TiO_2(r). Both catalysts had two main peaks with maxima at 590–650 K, and the H_2 uptake ended below 850 K. These results indicate that Co_3O_4 was first reduced to CoO, and subsequently to metallic Co, as discussed in an earlier report [32]. Since cobalt oxide was reduced completely below 850 K, the lowest reduction temperature of 973 K in this study was sufficiently higher than the temperature required to reduce the cobalt oxides completely.

The XP spectra and the XRD patterns suggested formation of an oxidized phase of cobalt in some catalysts investigated during the reaction; therefore, the oxidation behavior of the reduced catalyst in CO_2 was investigated. After Co/TiO_2(a) and Co/TiO_2(r) were reduced at 1023 K, the catalysts were treated in a CO_2/He (1:1) mixture at 1023 K. The XRD patterns after this treatment are shown in Figs. 6B and D for Co/TiO_2(a) and Co/TiO_2(r), respectively. It was found that the metallic cobalt in Co/TiO_2 was oxidized at 1023 K by CO_2 to form $CoTiO_3$, regardless of the TiO_2 phase composition. After this treatment, TPR measurements were carried out; the profiles are shown in Fig. 7C for Co/TiO_2(a) and in Fig. 7D for Co/TiO_2(r). Each profile had one peak at approximately 1000 K, indicating that reduction of $CoTiO_3$ had taken place for both Co/TiO_2(a) and Co/TiO_2(r). It should be noted that the reduction temperature of $CoTiO_3$ was much higher than that of Co_3O_4 (< 850 K). This implies that once $CoTiO_3$ is formed it is difficult to reduce under the reaction conditions.

4. Discussion

4.1. Catalytic behavior and causes of deactivation for the Co/TiO_2 catalysts

There is general agreement that catalytic deactivation during the CH_4/CO_2 reaction is caused by carbon deposition on active sites, sintering of metal particles, and oxidation of the metal [2]. In the present study, no carbon was detected (< 0.01 wt%) for any of the Co/TiO_2 catalysts. The cause of the deactivation for the Co/TiO_2 catalysts in this study is, therefore, metal oxidation and/or sintering of metal.

The reduction temperature had a strong influence on the catalytic behavior of Co/TiO_2(a) (Fig. 1). It was clearly shown that the Co/TiO_2(a) catalysts, reduced at 1123–1223 K, showed low activities for the reforming reaction (Fig. 1). At the beginning of the CH_4/CO_2 reaction (Fig. 2), CO_2 consumption for the Co/TiO_2(a) catalyst reduced at 1173 K (II) was much larger (complete CO_2 consumption within 10 s) than that for the Co/TiO_2(a) catalyst reduced at 1023 K (I). The reforming did not occur significantly over the Co/TiO_2(a) reduced at 1173 K, as seen by a small production of hydrogen and its complete loss within 1 min. It should be noted that the higher concentration of CH_4 com-

pared with CO_2 (or higher concentration of CO to H_2), for all of the catalysts, is ascribed to a preferential reverse water gas shift reaction ($CO_2 + H_2 \rightarrow CO + H_2O$) over reforming. However, in this case, the large CO_2 consumption is not due mainly to reforming, but to oxidation of the catalyst surface. It is assumed that the oxidation of the surface metal and the reforming reaction occur simultaneously. For the Co/TiO_2(a) catalyst reduced at 1023 K, reforming was faster than the oxidation, showing constant activity for reforming, and for the Co/TiO_2(a) catalyst reduced at 1173 K and Co/TiO_2(r) reduced at 1023 K, the oxidation of the metal was faster, resulting in a low activity for reforming.

XPS and XRD results give direct information about the surface state and the bulk state of the catalysts. In the Co 2*p* XP spectra (Fig. 4C and D) for Co/TiO_2(a) reduced at 1123 K, which showed fairly low activity toward the reaction, the metallic cobalt (777.4 eV) was oxidized during the reaction (broad peak at approximately 780.1 eV). It was reported that CoO, Co_3O_4, and $CoTiO_3$ have binding energies of cobalt at 780.0–780.5, 779.5–780.2, and 781.2 eV, respectively [33–36]. Although the exact species of cobalt cannot be clearly identified, the results obviously revealed that surface Co atoms in the catalysts were oxidized to Co^{2+} and/or Co^{3+} during the CH_4/CO_2 reaction. In addition, XRD patterns show the formation of a $CoTiO_3$ phase (Fig. 5 (II)). The XRD patterns still indicate the presence of metallic cobalt, even if the catalyst had lost all activity. However, sharp peaks of metallic cobalt were not observed, and peak intensities were lowered during the reaction, which confirms that the degree of sintering of metal was not significant. Therefore, it was assumed that the oxidation of metallic cobalt would occur at the surface of Co particles, as was confirmed by XPS, and that $CoTiO_3$ phase crystallization would proceed in the periphery between the metal and TiO_2. It is also assumed that Co in the core of the particles still remains metallic, as detected by XRD. Similar results for the Co/TiO_2(r) catalysts reduced at 973–1123 K were obtained by XRD analysis. Therefore, it was concluded from the kinetic measurements and the XPS and XRD results that low activities of Co/TiO_2(a) reduced at higher temperatures ($\geqslant$ 1123 K) and Co/TiO_2(r) can be attributed to rapid oxidation of the surface cobalt.

In contrast, the Co/TiO_2(a) catalysts reduced at 973–1073 K showed relatively high and stable activities (Fig. 1). However, a moderate decrease in catalytic activity was observed during the reaction. Metal sintering during the reaction was not significant compared with the decrease in activity (Table 2). Therefore, it is speculated that deactivation for these catalysts is due to both metal sintering and oxidation. The surface of metal particles can be oxidized slowly, and therefore the catalysts showed mild deactivation.

To confirm this idea, the Co/TiO_2(a) catalyst reduced at 1023 K was tested at different space velocities. The CH_4 conversion of the catalyst at a SV of 1200 ml g_{cat}^{-1} h^{-1} was higher than that at 6000 ml g_{cat}^{-1} h^{-1}, as expected (Fig. 3). Deactivation was observed especially at the beginning of the reaction and then gradually declined over time. XRD patterns of the catalyst after reaction indicate the metallic cobalt phase was retained during the reaction, but cobalt sintering occurred during the reaction, as was seen from a change in crystallite size from 26 to 38 nm. This degree of sintering and increase in crystallite size was much greater than that which occurred at a SV of 6000 ml g_{cat}^{-1} h^{-1} (26 to 32 nm). Therefore, the sintering of metal causes deactivation in this case. Although there are no additional data to reveal the causes and the incidental effects of sintering, it is suggested that the gas atmosphere of the latter part of the catalyst bed, where there are more products and fewer reactants, might have some influence on the catalyst, thereby accelerating sintering of the metal.

With regard to the reaction at a SV of 60,000 ml g_{cat}^{-1} h^{-1}, Co/TiO_2(a) reduced at 1023 K initially showed a 20% CH_4 conversion but was deactivated with time and completely lost catalytic activity within 20 h (Fig. 3). Formation of the $CoTiO_3$ phase after the reaction (Fig. 5 (II) (A′)) suggested that the metallic cobalt on TiO_2(a) was gradually oxidized with time. The degree of sintering was not significant (Table 2). Therefore, the main cause of complete deactivation would be oxidation of the metal. It can be assumed that higher SV provides the catalyst with more contact with the reactants (CO_2, CH_4). In this context, the inlet part of the catalyst in the reactor could be oxidized more easily because of a higher concentration of CO_2. On the other hand, metallic Co in the latter part of the catalyst bed is exposed to reductive products and could be sintered (as observed for the catalyst after the reaction at a SV of 1200 ml g_{cat}^{-1} h^{-1}). From this point, the cause of deactivation of the catalyst, reduced at 973–1073 K during reaction at a SV of 6000 ml g_{cat}^{-1} h^{-1}, is attributed to slow oxidation of metal from the front part of the catalyst bed and sintering of metal at the latter part of the catalyst bed.

4.2. Key parameters for the differences in catalytic behavior of the Co/TiO_2 catalysts

After calcination at 673 K (before reduction), Co_3O_4 was the only cobalt phase identified by XRD in the catalysts (Fig. 6A and C). In Fig. 7, the TPR spectra of Co/TiO_2(a) and Co/TiO_2(r) suggest that the lowest reduction temperature, 973 K, must be high enough to reduce all cobalt oxides in the catalysts. However, the Co 2*p* XP spectrum for Co/TiO_2(a) reduced at 1023 K showed a rather small peak attributed to an oxide phase of cobalt. Note that the TPR gave evidence that $CoTiO_3$ was less reducible than Co_3O_4 (Fig. 7). These results indicate that trace amounts of $CoTiO_3$ can be formed by calcination at 673 K and are not reduced by a reduction at 1023 K, although the amounts were too small to be detected by TPR and XRD analysis. This is in agreement with the report by Ho et al. [33] that surface $CoTiO_3$-like species, relatively less reducible, were formed in Co/TiO_2 by calcination at 673 K. However, because the catalyst reduced at lower temperature ($<$ 1123 K) showed

much higher activity than the catalyst reduced at higher temperature ($\geqslant$ 1123 K), it is concluded that the difference in the reduction degree of cobalt is not a crucial factor regarding catalytic behavior.

For the Co/TiO_2(a) catalysts reduced at 973–1073 K, which showed relatively high activity, and only moderate deactivation during the reaction, catalytic activities decreased with increasing reduction temperature (Fig. 1). Among these catalysts the cobalt crystallite size, phase composition of TiO_2, and the specific surface areas were very similar, and therefore the differences in activity are attributed to the amounts of cobalt available on the surface, which decreases with increasing reduction temperature (Table 2). The Co/TiO_2 catalysts have been reported as strong metal support interaction (SMSI) catalysts [37]. It has been reported for TiO_2-supported catalysts that the surface oxygen of TiO_2 could be removed in the range of the temperatures investigated ($\geqslant$ 773 K), and TiO_x species would be generated and cover the metal surface so that less CO chemisorption is detected. The possibility has also been discussed [3,12] that TiO_x species could block a large ensemble of metal particles that facilitate CH_4 decomposition and the resultant coke deposition. In addition, the generation of those TiO_x species would have a number of oxygen defect sites that enhance CO_2 dissociation and thus supply oxygen to the metal particles and therefore remove the surface carbon species. The synergistic effects of creating new active sites on CH_4/CO_2 reaction in the metal-support interfacial region will lead to an increase in turnover frequency (TOF) (s^{-1}) [12,13]. In this study, the dispersion was roughly estimated from the crystallite size from the following equation [37]:

$$D\ (\%) = 96.2/d,$$

where D (%) is the dispersion percentage of cobalt, and d is the particle size of cobalt, assuming an fcc structure for Co. This calculation resulted in $\approx$ 3% dispersion for all of the catalysts studied, which is more than 10 times larger than the values calculated from CO adsorption measurements (the highest dispersion is 0.36% for Co/TiO_2(a) reduced at 973 K) (Table 2). Therefore, it is confirmed that a higher reduction temperature increased the TiO_x coverage on metallic cobalt for the Co/TiO_2 catalysts, without increasing the metal crystallite size significantly. Strong resistance to coke deposition would be due to a small exposure of the cobalt surface, which destroys the large ensemble of metallic cobalt (coke deposition site) and creates active sites for reforming, especially CO_2 activation in the periphery of metal particles. In the current work, the TOF increased with increasing reduction temperature; for example, TOFs for CH_4 conversions after 1 h were estimated to be 4.0, 4.1, and 8.1 s^{-1} for the Co/TiO_2(a) catalysts reduced at 973, 1023, and 1073 K, respectively (TOFs were calculated from the molar flow rate of converted CH_4 divided by moles of CO adsorbed to the metal). However, TiO_x species may also block active metallic sites for reforming, and therefore the net value for conversions decreased with increasing reduction temperature (Fig. 1, Table 1).

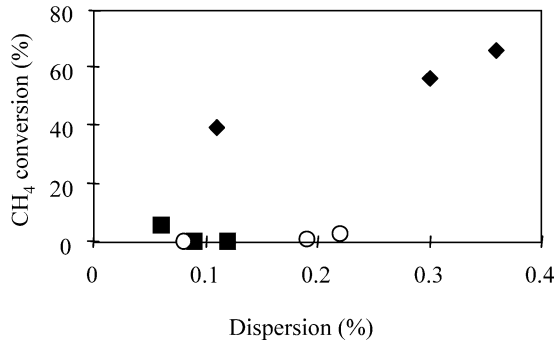

Fig. 8. CH_4 conversion at 1 h vs. dispersion of cobalt for the Co/TiO_2 catalysts reduced at different temperatures. (◆) Co/TiO_2(a) reduced at 973–1073 K; (■) Co/TiO_2(a) reduced at 1123–1223 K; (○) Co/TiO_2(r) reduced at 973–1123 K.

Compared with Co/TiO_2(a) reduced at 973–1073 K, the Co/TiO_2(a) catalyst reduced at 1123–1223 K and the Co/TiO_2(r) catalyst reduced at 973–1123 K showed low activities from the beginning of the reaction (Figs. 1 and 2). The metal crystallite sizes of Co/TiO_2(a) and Co/TiO_2(r) before the reaction (after reduction) were almost the same for these catalysts (Table 2). According to these results, the differences in the catalytic activity at the initial stage of the reaction were *not* attributed to the metal crystallite size. The relationship between CH_4 conversion and cobalt dispersion for the Co/TiO_2 catalyst is described in Fig. 8. As shown in this figure, low activities observed at the beginning of the reaction are *not* related to cobalt dispersion. The phase transfer from anatase to rutile was observed for the Co/TiO_2(a) catalyst at a reduction temperature of 1123 K (Fig. 5), and therefore the catalytic behavior seems to depend on the main TiO_2 structures, anatase or rutile. In other words, it is possible to say that the Co/TiO_2(a) catalyst, which retained the anatase phase, showed relatively high activity, whereas both Co/TiO_2(a), which obtained the rutile phase during reduction, and Co/TiO_2(r), originally supported on rutile phase, showed fairly low activity due to rapid oxidation of metallic Co to $CoTiO_3$.

Interestingly, the large differences in catalytic behavior are in accord with different TiO_2 phase compositions, that is, formation of $CoTiO_3$ is more favored on rutile than on anatase phase in a CH_4/CO_2 reaction. Hence, the $CoTiO_3$ formation rate under CO_2 treatment was compared for $CoTiO_2$(a) reduced at 1023 K and for Co/TiO_2(r) with the use of TPO with CO_2 (Fig. 9). Oxygen uptake was observed above 773 K for both catalysts. Co/TiO_2(a) gave a maximum at 1030 K, and Co/TiO_2(r), a maximum at 1100 K. The O/Co ratio, calculated from the net amount of oxygen uptake, was approximately in the range from 1.0 to 1.1. In addition, $CoTiO_3$ was the only cobalt species observed with XRD after these measurements (Figs. 6B and D). Therefore, the oxygen uptake would mainly correspond to the formation of $CoTiO_3$ ($Co + TiO_2 + CO_2 \rightarrow CoTiO_3 + CO$). Since

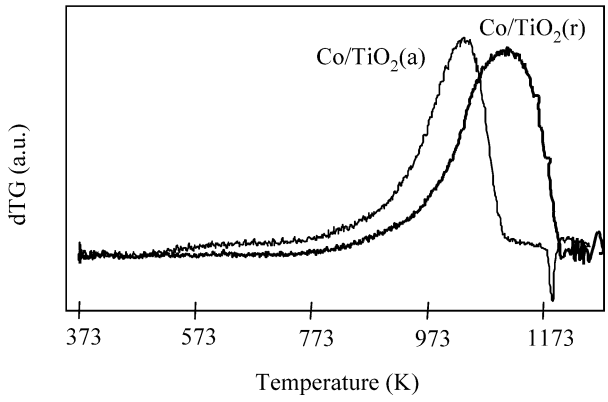

Fig. 9. Differential weight increase of Co/TiO_2(a) and Co/TiO_2(r) reduced at 1023 K flowing CO_2. Ramping rate: 10 K min^{-1}.

Co/TiO_2(a) had a lower temperature onset of the peak and peak maximum compared with Co/TiO_2(r), it can be suggested that Co/TiO_2(a) was more reactive with CO_2 than was Co/TiO_2(r) to form $CoTiO_3$. This tendency toward forming $CoTiO_3$ in CO_2 was different from that in the CH_4/CO_2 reaction, because the $CoTiO_3$ phase was formed more easily in Co/TiO_2(r) after the CH_4/CO_2 reaction than in Co/TiO_2(a). In other words, the tendency to form $CoTiO_3$ in CH_4/CO_2 cannot be predicted from the reactivity of Co supported on TiO_2 with only CO_2. Therefore, the difference in catalytic activities would correlate with the state of active sites (both metal and support participate) [3,4,19,21] on the catalyst surface and with the kinetics of the reactions with CH_4/CO_2 on those sites, where reductive (CH_4, H_2, CO) and oxidative (CO_2, H_2O) species coexist. When the reaction between these reductive and oxidative species keeps balance on the catalyst surface, no carbon deposition or oxidation of metal occurs, and accordingly the catalyst exhibits an extended life. For the Co/TiO_2 catalysts, the $CoTiO_3$ phase is formed by oxidative species when the CH_4/CO_2 reaction is not balanced. Once formed, the $CoTiO_3$ phase is difficult to reduce, and the catalyst becomes inactive toward the reforming reaction.

Anatase and rutile structures are different in the surface structures and chemical properties, such as facets of the surface, acid–base properties, the degree of oxygen vacancies, etc. Such factors can directly affect the reaction between reductive and oxidative species in reforming. As a result, anatase-type TiO_2 comparatively keeps the surface cobalt in the metal state and gives the catalyst relatively stable activity, whereas rutile-type TiO_2 induces rapid oxidation of cobalt and provides very low activities from the beginning of the reaction.

5. Conclusion

Influence of the reduction temperature on Co/TiO_2 catalysts was investigated for the CO_2 reforming of CH_4. Differences in the reduction temperature significantly affect the catalytic behavior of Co/TiO_2. Remarkably, all of the Co/TiO_2 catalysts showed strong resistance for coke deposition (< 0.01 wt%) in the CH_4/CO_2 reaction at 1023 K. The catalysts reduced at relatively lower temperatures (973–1073 K), where TiO_2 retained the anatase phase, had relatively high and stable activities. On the other hand, the Co/TiO_2 catalysts, where the anatase phase was mainly transformed to the rutile phase by reduction at higher temperatures (1123–1223 K) or where the cobalt was supported on the rutile phase, showed fairly low activities from the beginning of the reaction. Both kinetic measurements and characterization with XPS and XRD techniques revealed that low activities are ascribed to rapid oxidation of metallic cobalt. Since the differences in catalytic activity cannot be correlated with the differences in Co dispersion and Co crystallite sizes, it is suggested that the large difference in the initial activities could be ascribed to the differences in the TiO_2 bulk crystal structure. As a result, oxidation of cobalt supported on rutile is more favored than that of cobalt supported on anatase during CH_4/CO_2 reforming. This indicates that TiO_2, together with Co, strongly participates in the reaction and is of importance to the optimization of a balance between CH_4 and CO_2. Knowledge obtained from this study, for example, the influence of reduction temperature and TiO_2 phase composition on the catalytic behavior of TiO_2-supported catalysts, can be judiciously applied.

Acknowledgment

The authors thank Dr. K. Inazu for his help with XPS measurements.

References

[1] J.R. Rostrup-Nielsen, in: J.R. Anderson, M. Boudart (Eds.), Catalysis, Science and Technology, vol. 5, Springer, Berlin, 1984, Chapter 1.
[2] M.C.J. Bradford, M.A. Vannice, Catal. Rev. Sci. Eng. 41 (1999) 1, and literature cited therein.
[3] M.C.J. Bradford, M.A. Vannice, Appl. Catal. A 142 (1996) 97.
[4] J.H. Bitter, K. Seshan, J.A. Lercher, J. Catal. 176 (1998) 93.
[5] J.R. Rostrup-Nielsen, J. Catal. 33 (1974) 184.
[6] O. Yamazaki, T. Nozaki, K. Omata, K. Fujimoto, Chem. Lett. 0 (1992) 1953.
[7] E. Ruckenstein, H.Y. Wang, Appl. Catal. A 204 (2000) 257.
[8] E. Ruckenstein, H.Y. Wang, J. Catal. 205 (2002) 289.
[9] A. Erdöhelyi, J. Cserényi, F. Solymosi, J. Catal. 141 (1993) 287.
[10] Z. Zhang, V.A. Tsipouriari, A.M. Efstathiou, X.E. Verykios, J. Catal. 158 (1996) 51.
[11] M.C.J. Bradford, M.A. Vannice, Appl. Catal. A 142 (1996) 73.
[12] M.C.J. Bradford, M.A. Vannice, Catal. Lett. 48 (1997) 31.
[13] T. Osaki, J. Chem. Soc., Faraday Trans. 93 (1997) 643.
[14] K. Nagaoka, M. Okamura, K. Aika, Catal. Commun. 2 (2001) 255.
[15] K. Nagaoka, K. Takanabe, K. Aika, Chem. Commun. (2002) 1006.
[16] K. Nagaoka, K. Takanabe, K. Aika, Appl. Catal. A 255 (2003) 13.

[17] K. Nagaoka, K. Takanabe, K. Aika, Appl. Catal. A 268 (2004) 151.
[18] Z.L. Zhang, V.A. Tsipouriari, A.M. Efstathiou, X.E. Verykios, J. Catal. 158 (1996) 51.
[19] A.N.J. van Keulen, K. Seshan, J.H.B.J. Hoebink, J.R.H. Ross, J. Catal. 166 (1997) 306.
[20] M.E.S. Hegarty, A.M. O'Connor, J.R.H. Ross, Catal. Today 42 (1998) 225.
[21] K. Nagaoka, K. Seshan, J.A. Lercher, K. Aika, Catal. Lett. 70 (2000) 109.
[22] K. Nagaoka, K. Seshan, K. Aika, J.A. Lercher, J. Catal. 197 (2001) 34.
[23] S.J. Tauster, S.C. Fung, R.T. Garten, J. Am. Chem. Soc. 100 (1978) 170.
[24] S.J. Tauster, S.C. Fung, R.T.K. Baker, J.A. Horsley, Science 211 (1981) 1121.
[25] S.A. Stevenson, G.B. Raupp, J.A. Dumesic, S.J. Tauster, R.T.K. Baker, in: S.A. Stevenson, J.A. Dumesic, R.T.K. Baker, E. Ruckenstein (Eds.), Metal–Support Interactions in Catalysis, Sintering, and Redispersion, Van Nostrand Reinhold, New York, 1987, p. 3.
[26] D.J.C. Yates, J. Phys. Chem. 65 (1961) 746.
[27] D.D. Beck, J.M. White, C.T. Ratcliffe, J. Phys. Chem. 90 (1986) 3123.
[28] M.R. Prairie, A. Renken, J.G. Highfield, K.R. Thampi, M. Grätzel, J. Catal. 129 (1991) 130.
[29] G. Ramis, G. Busca, V. Lorenzelli, J. Chem. Soc., Faraday Trans. 83 (1987) 1591.
[30] V.S. Lusvardi, M.A. Barteau, W.E. Farneth, J. Catal. 153 (1995) 41.
[31] H.P. Klug, L.E. Alexander, X-Ray Diffraction Procedures, Wiley, New York, 1974.
[32] J.H.A. Martens, H.F.J. van't Blik, R. Prins, J. Catal. 97 (1986) 200.
[33] S.-W. Ho, J.M. Cruz, M. Houalla, D.M. Hercules, J. Catal. 135 (1992) 173.
[34] R. Riva, H. Miessner, R. Vitali, G. Del Piero, Appl. Catal. A 196 (2000) 111.
[35] Y. Brik, M. Kacimi, M. Ziyad, F. Bozon-Verduraz, J. Catal. 202 (2001) 118.
[36] M. Voß, D. Borgmann, G. Wedler, J. Catal. 212 (2002) 10.
[37] R.C. Reuel, C.H. Bartholomew, J. Catal. 85 (1984) 63.